W-Boson Production at Upgraded HERA in the Standard Model and Beyond

M.N.Dubinin

Institute of Nuclear Physics, Moscow State University

119899 Moscow, Russia

H.S.Song

Center for Theoretical Physics, Seoul National University

Seoul, 151-742, Korea

Abstract

Event characteristics of W boson production at HERA collider are untrivial and sensitive to the production mechanisms. We calculate the distributions of the four particle final state defined by the complete set of W producing perturbative leading order diagrams in the Standard Model and its extension with anomalous effective lagrangian in the gauge sector.

It is very important to understand in details the mechanisms of W-boson production at upgraded HERA ($L \sim 200$ pb^{-1}/year, $\sqrt{s} = 314$ GeV). The number of W-production events will be large enough both in leptonic and hadronic W decay channels, giving potentially large backgrounds to the signals of new physics [1], including contact interactions, leptoquarks and R-parity conserving or violating SUSY processes. At the same time if the weak current couplings of gauge bosons are measured with the accuracy of 10^{-4} [2], the accuracy of anomalous couplings restriction in the gauge boson sector is of order 1 only [3], so the self-interaction of vector bosons is not experimentally fixed at comparable level of precision.

The complete set of 10 tree level diagrams for the process of W-boson production $e^-p \to e^-\mu^+\nu_\mu X$ is shown in Fig.1. In the simpler $2 \to 3$ process

approximation [4] of W-boson on-shell $M_{\mu\nu} = (p_\nu + p_\mu)^2 = m_W^2$ we have to keep seven s-channel diagrams with an outgoing W boson line and omit ladder diagrams 1,6 and 7. However this approximation of infinitely small W width $\Gamma_{tot}^2/[(M_{\mu\nu} - m_W)^2 + \Gamma_{tot}^2] = \pi\delta(M_{\mu\nu} - m_W)\Gamma_{tot}$, being rather satisfactory for the calculation of total W production rate, is not sufficient for the analysis of final muon distributions and other delicate features of event topology, like spin correlations. Taking W boson off-shell $W \to \mu\nu_\mu$ in the $2 \to 4$ process approximation requires ladder graphs 1,6,7 in order to preserve gauge invariance [5].

Main contribution to the cross section comes from diagram 3 containing photon and quark t-channel propagators. When the t-channel gamma and quark are close to mass shell the QCD corrections are large, potentially developing a nonperturbative regime of 'resolved photon' [6]. The kinematical configurations of resolved photon are separated by a cut near t-channel quark pole $\Lambda^2 = (p_q - p_W)^2$. 'Resolved' W-production is not more than a quark-antiquark fusion where one of the quarks appears as a constituent of gamma and another one as a constituent of proton. Existing parametrizations of quark distributions inside gamma (measured in $\gamma\gamma$ collisions) seem to be not as precise as PDF in proton, so the resolved W-production cannot be calculated with the same reliability [7] as the perturbative leading order (also called 'direct') contribution of ten diagrams in Fig.1. The contribution of resolved part is of order 10% W-production cross section. In the following we shall discuss the distributions corresponding to direct (perturbative leading order) part of the W production amplitude in the Standard Model and beyond [7].

Calculation of the leading order amplitude (ten diagrams in Fig.1) was performed by means of CompHEP package [8]. We used the 'overall' prescription [5] for vector boson propagators. Electron mass was kept nonzero for the regularization of t-channel gamma pole. Numerical level cancellation of the $1/Q^4$ gamma propagator pole in the separately taken squared diagrams to the $1/Q^2$ pole in the entire amplitude, required by the gauge invariance, can be demonstrated explicitly [7].

We show the event characteristics of the process $e^- p \to e^- \mu^+ \nu_\mu X$ in Figs.2-4 (proton structure functions MRS A [9]). First row of plots in each figure represents the distributions of the electron, second row of plots - distributions of the (anti)muon, and third row of plots shows the distributions of the final quark (of course all partonic subprocesses contributing to W

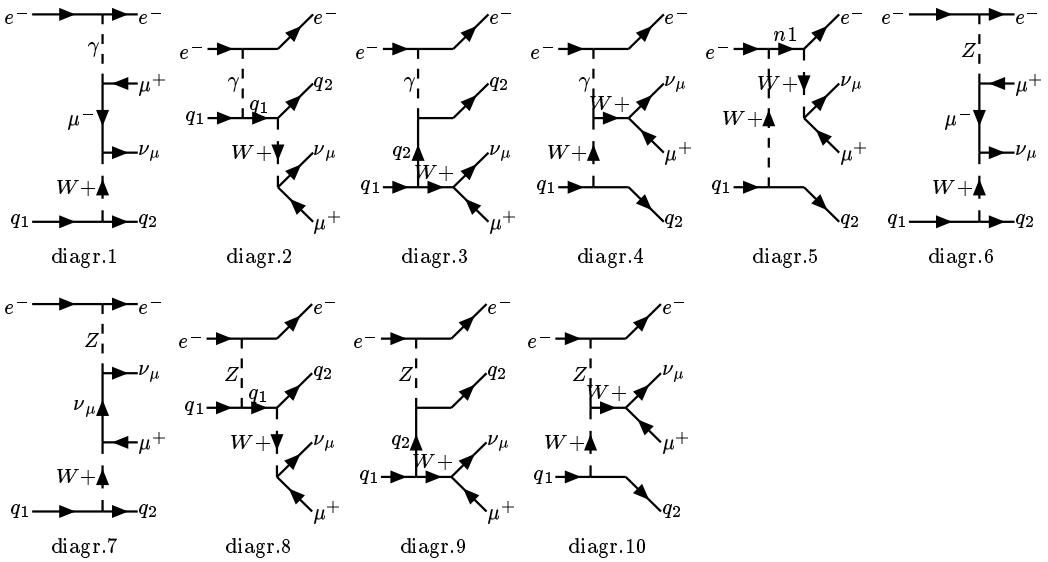

Figure 1: Feynman diagrams for the process $e^- q_1 \to e^- \mu^+ \nu_\mu q_2$

production are summed). Different cuts for t-channel quark momentum $\Lambda^2 = (p_q - p_W)^2$ were imposed for the calculation of event characteristics in Fig.2 and Fig.3, where Λ is equal to 0.2 GeV and 5 GeV, correspondingly. The distributions in Fig.4 were calculated at $\Lambda = 5$ GeV with the additional 20 GeV cut around the W pole: $M_W - 20$ GeV $\leq M(\mu\nu_\mu) \leq M_W + 20$ GeV. This cut is used in the EPVEC generator [5], so the distributions in Fig.5 are calculated with the same cuts as in [10]. Soft muons in the distributions $d\sigma/dE_\mu$ and $d\sigma/dp_{T\mu}$ come from the ladder diagrams 1,6,7 in Fig.1. Jets at the angle 180 degrees with the proton beam appear from diagram 3, Fig.1, when the quasireal photon produces a quark-antiquark pair collinear to the initial electron. We can see that the backscattered jet peak is sensitive to the value of Λ cut and gradually goes down as we increase it. But very probably this decrease of direct contribution is more or less compensated by the 'photon remnant' in the contribution from the resolved part. Muons at 180 degree with the proton beam appear at any value of Λ - only the shape of $d\sigma/dE_\mu$ is slightly affected and the normalization is changed. Kinematical cut around the W-pole implemented in 'canonical' EPVEC removes soft muons and muons at 180 degree with the beam completely.

In the muonic channels the total cross section is equal approximately to 150-160 fb, giving about 35 events/year at the integrated luminosity 200 pb^{-1}. Additional kinematical cuts are necessary in the electron channels for separation of misidentification backgrounds, and the number of identifiable events from $W \to e\nu_e$ is slightly smaller. In total at upgraded HERA collider it could be possible to observe about 60 W-production events/year. At present time HERA luminosity is too small to produce a number of W sufficient for a quantitative analysis. Presently available H1 data [11] shows one event in the electron channel (2.4 events expected) and two events in the muon channel (0.8 events expected), with the topology compatible with W production processes (three more H1 events in the muon channel have the kinematic properties different from those given by W production mechanisms). ZEUS data [12] shows three events in the electron channel and none of the events passes through kinematical cuts in the muon channel.

Some uncertainty in the normalization of total cross section exists for the reason of possibly large QCD corrections in the phase space region near the t-channel quark pole. Recent calculations [13] of QCD corrections to the dominant resolved photoproduction process seem to show the NLO correction factor of 48% (although the kinematical cut of the standard deep inelastic Q^2 variable was used instead of Λ^2 cut in that calculations).

Anomalous U(1)-gauge-invariant, C and P-parity-conserving effective lagrangian in the gauge sector can be taken in the form [14]

$$L_{eff} = g_V(W^+_{\mu\nu}W^{\mu}V^{\nu} - W^{\mu\nu}W^+_{\mu}V_{\nu} + k\ W^+_{\mu}W_{\nu}V^{\mu\nu} + \frac{\lambda}{m^2_W}W^+_{\rho\mu}W^{\mu}_{\ \nu}V^{\nu\rho}) \quad (1)$$

where $g_\gamma = e$ and $g_Z = ecos\vartheta_W/sin\vartheta_W$, $W_{\mu\nu} = \partial_\mu W_\nu - \partial_\nu W_\mu$, $V_{\mu\nu} = \partial_\mu V_\nu - \partial_\nu V_\mu$. Spatial structure of the fourth term in the lagrangian of dimension six is multiplied by m_W^{-2} factor, so parameters λ and k are dimensionless. The reasons to express the value of λ in the units of m_W are probably historical, it would be more natural to use some energy scale of new physics phenomena instead of W mass. We show one of the distributions calculated using the anomalous effective lagrangian (1) in Fig.5.

Taking into account some typical detector experimental cuts nesessary for the separation of misidentification backgrounds and realistic experimental acceptancies we can derive the following limits for Δk and λ, giving the observable deviation of total cross section from the Standard Model value at

68% and 95% confidence level:

$$-1.70 < \lambda < 1.70, \qquad -1.05 < \Delta k < 0.48, \qquad 68\% \quad CL$$
$$-2.24 < \lambda < 2.24, \qquad \Delta k < 0.89, \qquad 95\% \quad CL$$

at the integrated luminosity 200 pb^{-1}, and

$$-1.03 < \lambda < 1.03, \qquad -0.31 < \Delta k < 0.27, \qquad 68\% \quad CL$$
$$-1.75 < \lambda < 1.75, \qquad -0.58 < \Delta k < 0.46, \qquad 95\% \quad CL$$

at the integrated luminosity 1000 pb^{-1}. The limits from Tevatron collider available at present time [3] are close to the possible upgraded HERA limits at the luminosity 1000 pb^{-1}.

One of the authors (M.D.) is grateful to M.Kuze, E.Perez, D.Waters and R.Walczak for useful discussions.

References

[1] H1 Collaboration, ICHEP98, XXIX Int. Conf. on High Energy Physics, Vancouver, 23-29 July 1998, abstracts 579, 580, 581, 584

ZEUS Collaboration, ICHEP98, XXIX Int. Conf. on High Energy Physics, Vancouver, 23-29 July 1998, abstracts 753, 754, 758, 759

[2] Particle Data Group, Phys.Rev. D54 (1996) 1

[3] S.Abachi et al, D0 Collaboration, Phys.Rev.Lett., 78 (1997) 3634

[4] U.Baur, D.Zeppenfeld, Nucl.Phys. B325 (1989) 253

[5] U.Baur, J.Vermaseren, D.Zeppenfeld, Nucl.Phys. B375 (1992) 3

[6] M.Drees, Mod.Phys.Lett., A2 (1987) 573
J.Blümlein, G.Schuler, in:*Proc.of Snowmass Summer Study on Research Directions for the Decade*, 1990

[7] M.N.Dubinin, H.S.Song, Phys.Rev. D57 (1998) 2927

[8] E.Boos, M.Dubinin, V.Ilyin, A.Pukhov, V.Savrin, preprint INP MSU 94-36/358, 1994 (hep-ph/9503280)
in: *Proc.of X Workshop on High Energy Physics and Quantum Field Theory*, ed.by B.Levtchenko, V.Savrin, Moscow, 1996, p.101

[9] A.D.Martin, W.J.Stirling, R.G.Roberts, Phys.Rev. D51 (1995) 4756

[10] V.Noyes, in: *Proc.of the Workshop on Future Physics at HERA 1995/96*, ed.by G.Ingelman, A.De Roeck and R.Klanner, p.190

[11] H1 Collaboration, ICHEP98, XXIX Int. Conf. on High Energy Physics, Vancouver, 23-29 July 1998, abstract 578

H1 Collaboration, DESY preprint 98-063

[12] ZEUS Collaboration, ICHEP98, XXIX Int. Conf. on High Energy Physics, Vancouver, 23-29 July 1998, abstract 756

[13] M.Spira, talk on the WG80 meeting of DESY Workshop 'Monte Carlo generators for HERA physics', September 1998

[14] K.Hagiwara, R.D.Peccei, D.Zeppenfeld, K.Hikasa, Nucl.Phys. B282 (1987) 253

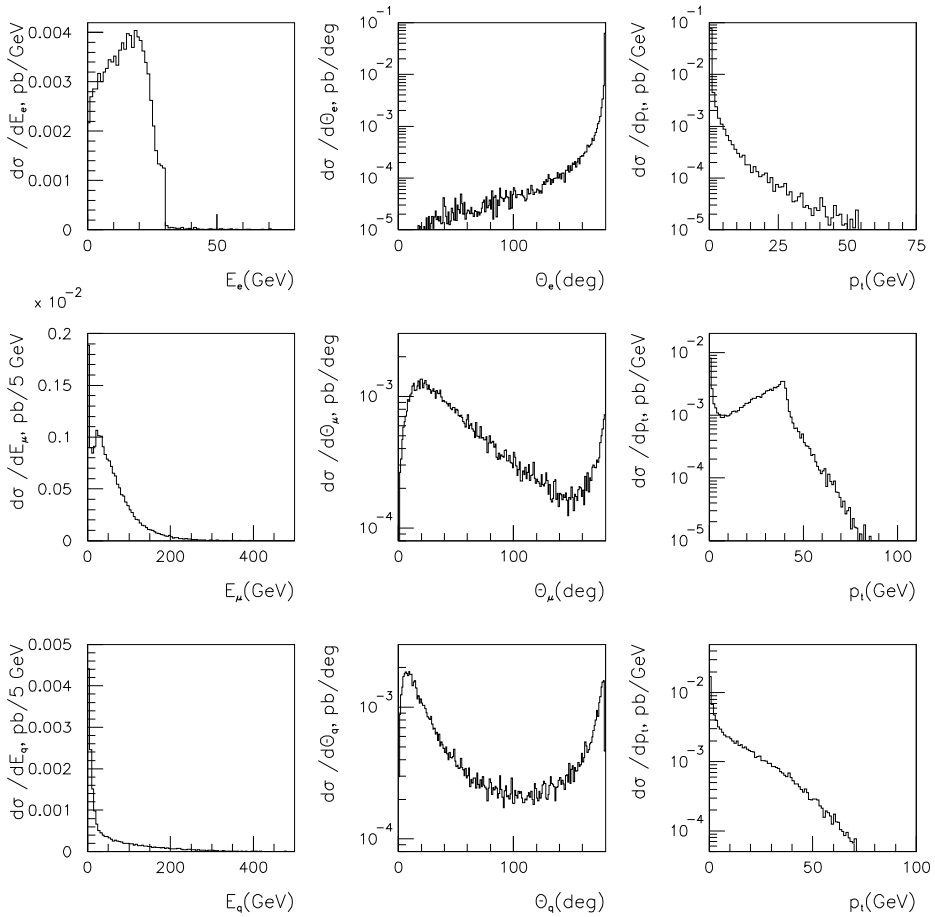

Figure 2: First row of plots - distributions of the electron energy, scattering angle and transverse momentum in the process $e^- p \to e^- \mu^+ \nu_\mu X$. Second row of plots - distributions of the muon energy, muon scattering angle and transverse momentum. Third row of plots - distributions of the quark energy, angle and transverse momentum for the same process. Total cross section 92.1 fb, t-channel quark cut $\Lambda = 0.2$ GeV.

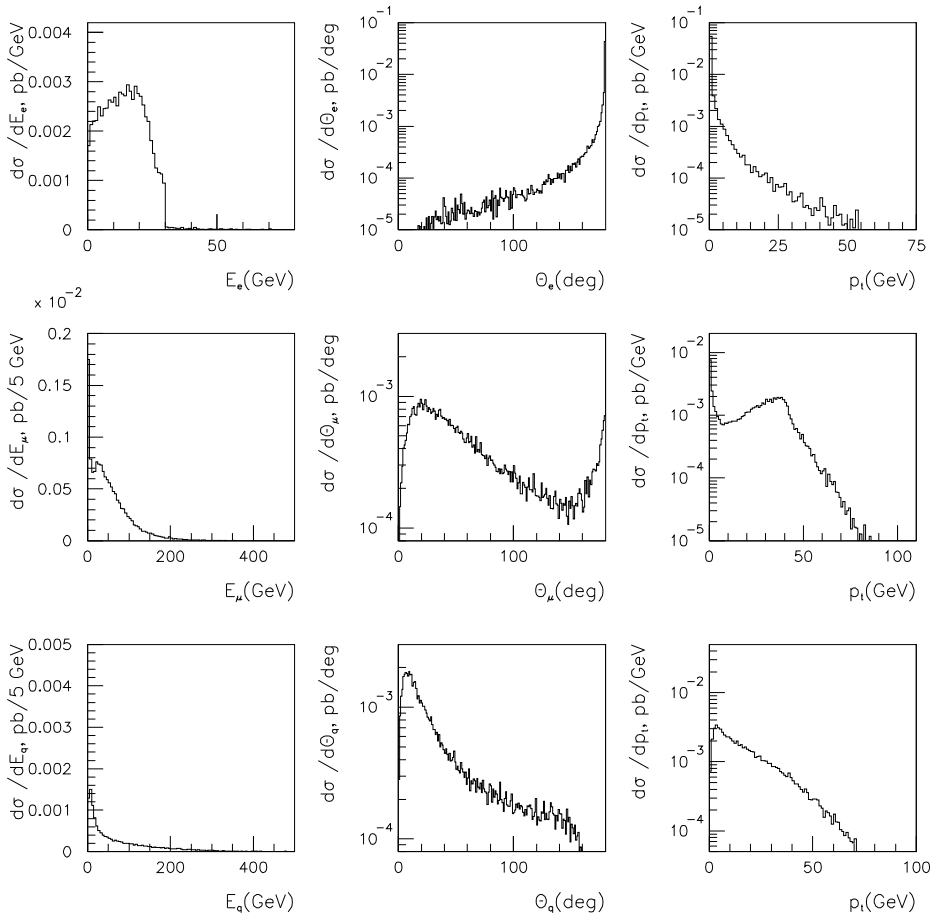

Figure 3: First row of plots - distributions of the electron energy, scattering angle and transverse momentum in the process $e^- p \to e^- \mu^+ \nu_\mu X$. Second row of plots - distributions of the muon energy, muon scattering angle and transverse momentum. Third row of plots - distributions of the quark energy, angle and transverse momentum for the same process. Total cross section 68.6 fb, t-channel quark cut $\Lambda = 5$ GeV.

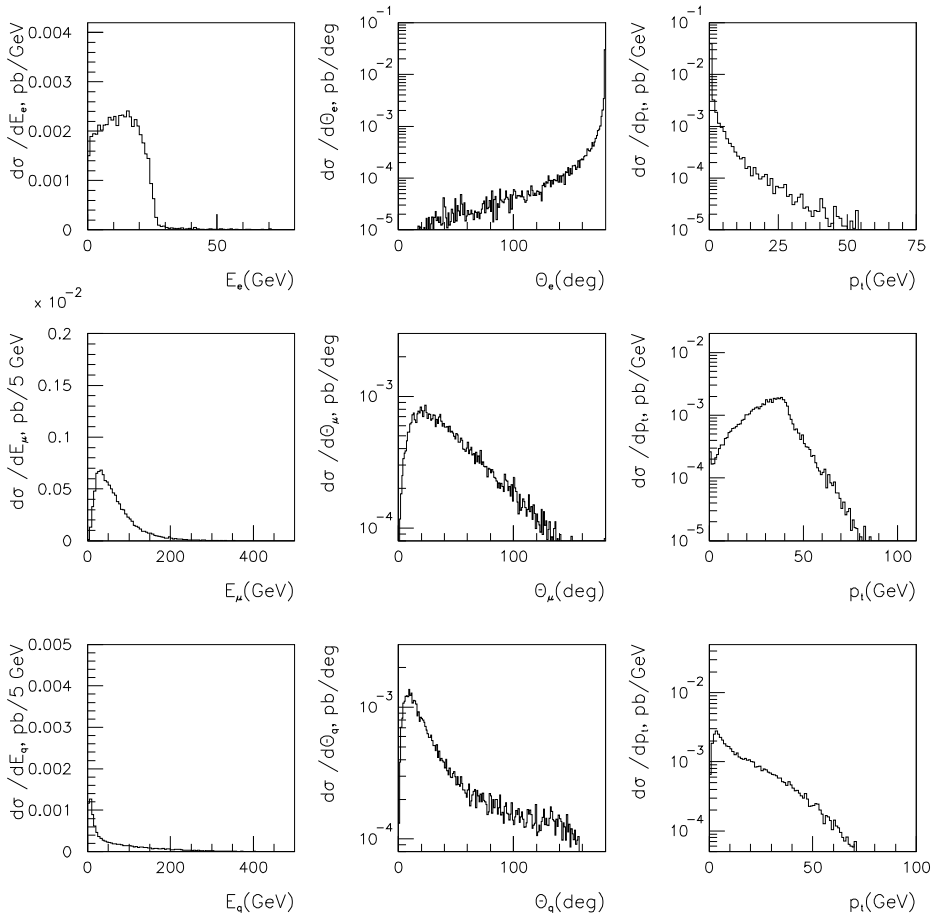

Figure 4: First row of plots - distributions of the electron energy, scattering angle and transverse momentum in the process $e^- p \to e^- \mu^+ \nu_\mu X$. Second row of plots - distributions of the muon energy, muon scattering angle and transverse momentum. Third row of plots - distributions of the quark energy, angle and transverse momentum for the same process. Total cross section 51.7 fb, t-channel quark cut $\Lambda = 5$ GeV, the cut around the W pole 20 GeV, to be compared with the same distributions obtained by means of EPVEC generator, see [10]

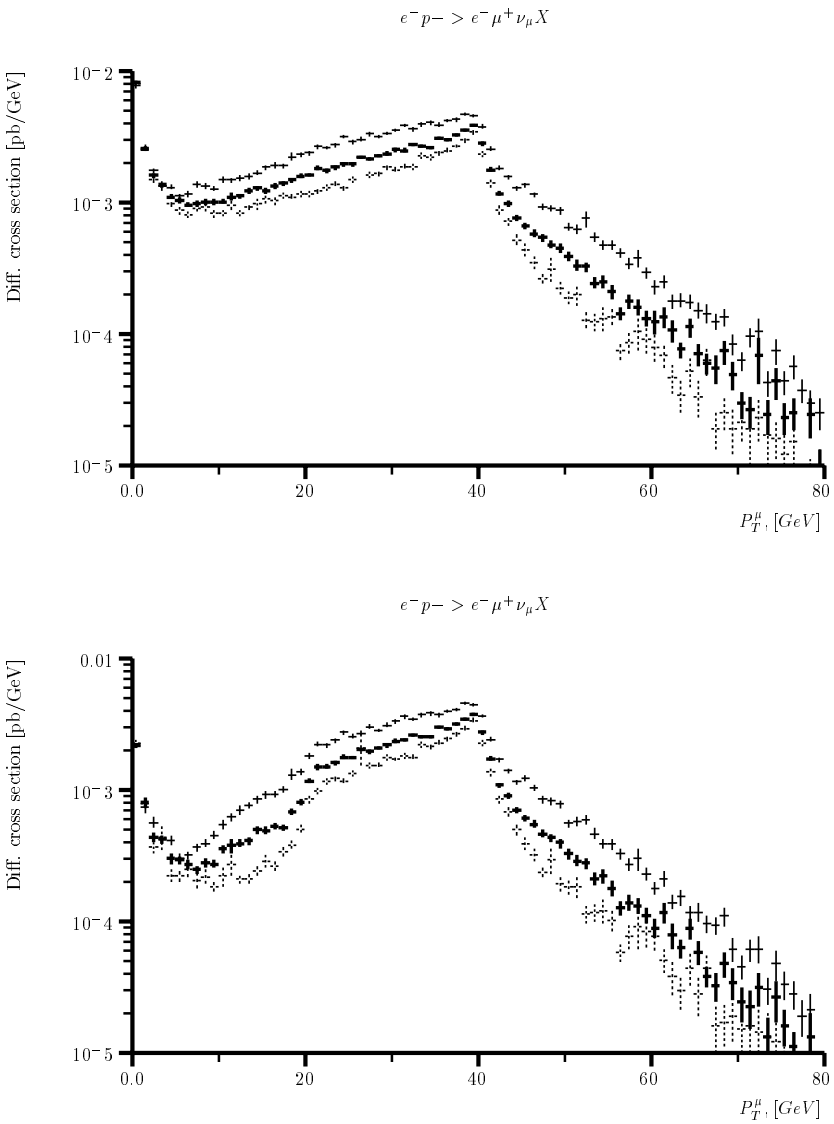

Figure 5: Distribution of muon transverse momentum in the reaction $e^-p \to e^-\mu^+\nu_\mu X$. Upper plot: no kinematical cuts, solid lines - standard case, dash lines - anomalous three vector boson couplings case, $\lambda = 0$, $k = 0$, thin solid lines - $\lambda = 0$, $k = 2$. Lower plot: the same distributions after the detector kinematical cuts $E_\mu \geq 10$ GeV, missing $p_T \geq 20$ GeV.